Available online at www.sciencedirect.com

ScienceDirect

Physics Procedia 74 (2015) 212 – 219

Physics Procedia

Conference of Fundamental Research and Particle Physics, 18-20 February 2015, Moscow, Russian Federation

# The counting and triggers signals formation system for gamma-telescope GAMMA-400

I.V. Arkhangelskaja[a,*] , A.I. Arkhangelskiy[a], E.N. Chasovikov[a], A.M. Galper[a,b], M.D. Kheymits[a], A.E. Murchenko[a], Y.T. Yurkin[a]

[a]*National Research Nuclear University MEPhI (Moscow Engineering Physics Institute),Kashirskoe Shosse 31, Moscow 115409, Russia*
[b]*Lebedev Physical Institute, Russian Academy of Sciences, Leninskiy prospekt 53, Moscow, 119991, Russia*

**Abstract**

Gamma-telescope GAMMA-400 consists of anticoincidence system (polyvinylyltoluene BC-408 based top and lateral detector sections, the converter-tracker with thickness of ~1 $X_0$ (where $X_0$ is radiation length), time-of-flight system (two sections composed of BC-408 detectors with 50 cm distance between), two calorimeters makes of CsI(Tl) crystals (position-sensitive and electromagnetic. Also it includes neutron detector, two BC-408 based scintillation detectors of the calorimeter, and four BC-408 based lateral detectors of the calorimeter. The total calorimeter thickness is 25 $X_0$ or 1.2 $\lambda_0$ for vertical incident particles registration and 54 $X_0$ or 2.5 $\lambda_0$ for laterally incident ones (where $\lambda_0$ is nuclear interaction length). The counting and triggers signals formation system started the data acquisition and provides particle identification. It used 2 pulses types: fast (t≤10 ns) from BC-408 based scintillation detectors and slow (t≤10 ms) from inorganic ones. Also fast pulses (t~10 ns) from inorganic calorimeters individual detectors amplitude discriminators are included to this system information processing. Only signals from each detectors system individual detecting units without any summation are used for particle identification. The relationship between γ-quanta and relativistic particles (electrons and protons) energy deposition in GAMMA-400 detectors are discussed. The onboard triggers and trigger markers formation algorithms are described jointly with particles identification methods.

Peer-review under responsibility of the National Research Nuclear University MEPhI (Moscow Engineering Physics Institute)

*Keywords:* partiles identification, particles rejection, gamma-astronomy; cosmic rays

## 1. GAMMA-400 short description

At present, the high-energy gamma-ray astronomy outside the Earth's atmosphere progress is connected with Fermi Gamma-ray Space Telescope (formerly GLAST) - see, for example, [1] launched in June, 2008 into the

* Corresponding author. Tel.: +7-916-668-5051.
*E-mail address:* irene.belousova@usa.net


Peer-review under responsibility of the National Research Nuclear University MEPhI (Moscow Engineering Physics Institute)
doi:10.1016/j.phpro.2015.09.201

approximately circular near-Earth orbit with initial altitude of ~565 km. It intended to registration of γ-ray emission in the energy range from several keV (Glast Burst Monitor - GBM) to >300 GeV (Large Area Telescope - LAT). This apparatus used for studying of charged particles acceleration mechanisms in the astrophysics sources (active galaxies nuclei, pulsars, supernovae and so on); definition of the unidentified EGRET sources nature; detailed galactic and extragalactic diffuse γ-ray emission investigation, gamma-ray bursts (GRB) search and analysis; research of a dark matter and so on [1 - 3].

The next important step in the understanding of variable active astrophysical objects occurring processes nature will be obtaining the results by high-energy gamma-ray telescopes with better angular and energy resolutions than Fermi/LAT.

GAMMA-400 ((Gamma Astronomical Multifunctional Modular Apparatus) will be the new generation satellite γ-observatory with the following main scientific goals [4 - 7]: indirect dark matter origin study by the gamma-ray astronomy methods, discrete astrophysical sources observations, diffuse background γ-emission investigations, high energy GRB emission research, the study of high energy e−e+ fluxes, research of high energy light nuclei fluxes.

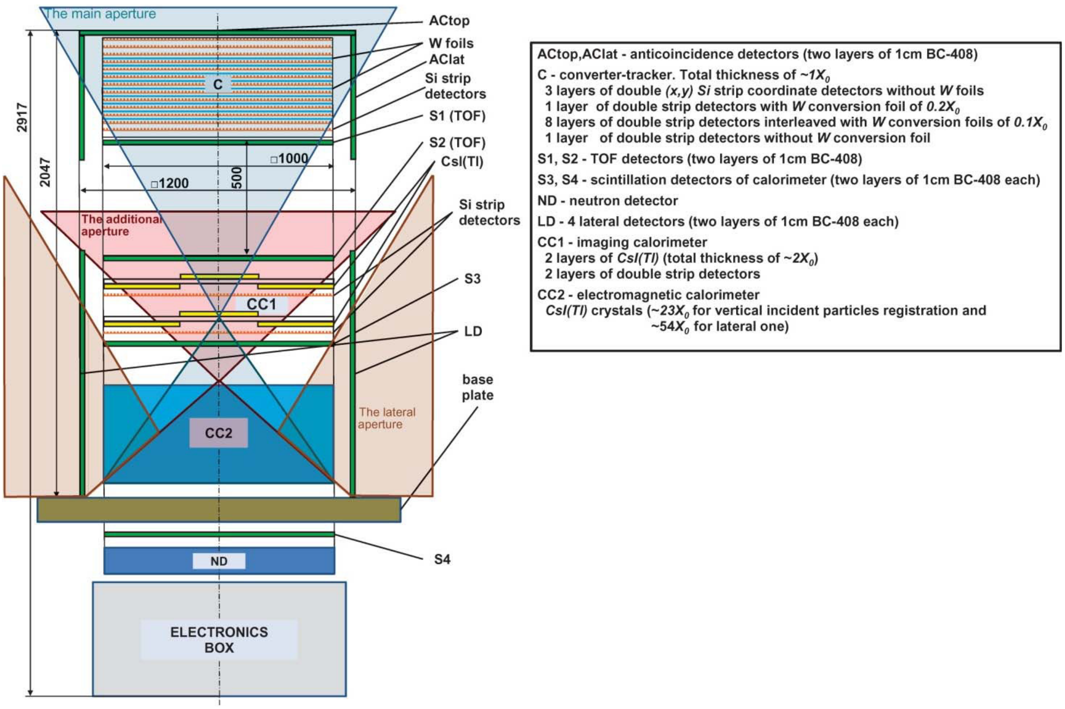


Fig. 1. The physical scheme of the gamma-telescope GAMMA-400 with three apertures for particles registration.

Gamma-telescope GAMMA-400 physical scheme is shown at Fig. 1. Gamma-telescope GAMMA-400 consists of anticoincidence system (BC-408 based top and lateral sections - ACtop and AClat), the converter-tracker (C), time-of-flight system (2 sections S1 and S2 composed of BC-408 detectors), position-sensitive calorimeter CC1 makes of 2 strips layers (pitch of 0.08 mm) and 2 layers of CsI(Tl) detectors, electromagnetic calorimeter CC2 composed of CsI(Tl) crystals, neutron detector ND, BC-408 based scintillation detectors of the calorimeter (S3 and S4), BC-408 based lateral detectors of the calorimeter (LD) [4, 5 - 7]. All BC-408 based detector systems consist of 2 sensitive layers of 1 cm thickness each. The converter-tracker is composed of 13 layers of double (x, y) silicon strip coordinate detectors (pitch of 0.08 mm) [5]. The first three and final one layers are without tungsten while the middle nine layers are preceded with tungsten conversion foil each: the first one with thickness 0.2 $X_0$ and the next eighth with 0.1 $X_0$ one (where $X_0$ is radiation length). The thickness of CC1 and CC2 is 2 $X_0$ (0.1 $\lambda_0$) and 23 $X_0$ (1.1 $\lambda_0$) respectively (where $\lambda_0$ is nuclear interaction length). The total calorimeter thickness is 25 $X_0$ or 1.2 $\lambda_0$ for vertical incident particles registration and 54 $X_0$ or 2.5 $\lambda_0$ for laterally incident ones.

Together with the γ-telescope GAMMA-400, the space observatory will include non shown at Fig. 1 devices: two star sensors for determining the GAMMA-400 axes with accuracy of approximately 5", two magnetometers, and the KONUS-FG gamma-ray burst monitor (4 position and 2 spectrometric detectors) [5].

Three apertures provide events registration both from upper and lateral directions. The main aperture provides the best angular (all strip layers information analysis) and energy (energy deposition in the all detectors studying) resolution. Gamma-telescope GAMMA-400 is optimized for the gamma-quanta and charged particles with energy $\sim 1.0\times10^2$ GeV detection with the best parameters in the main aperture [4 - 6, 8]: the angular resolution ~0.01°, the energy resolution ~1%, and the proton rejection factor $\sim 5\times10^5$. In addition, GAMMA-400 is able to registered gamma-rays and electrons (positrons) in the energy range from $0.1–3.0\times10^3$ GeV in the main aperture. Also this aperture allows investigating high energy light nuclei fluxes characteristics. The GAMMA-400 effective area in the main aperture is ~4000 $cm^2$ at $E\gamma > 1$ GeV. Both additional and lateral apertures energy resolution is ~2% for electrons, positrons, light nuclei and gamma-quanta in energy range E>10 GeV.

For events registered in the additional aperture, the angular resolution is provided by strip layers in the CC1 and for gamma-quanta is from $\sim 5^o$ to $\sim 4^o$ in energy range 1.0 MeV - 0.1 GeV and from $\sim 4^o$ to $\sim 0.7^o$ for 0.1 - 1.0 GeV one. For particles with E >1.0 the angular resolution is $\sim 0.7^o$. The additional aperture energy resolution provides due to energy deposition analysis in S2, S3, S4, LD and calorimeters (CC1 and CC2).

Gamma-quanta, electrons/positrons and light nuclei with energy E>10 GeV also registered in the lateral aperture. This aperture allows detecting of low-energy gammas in the range 0.2 - 10 MeV and photons with energy of 10 MeV – 10 GeV. The energy resolutions in these cases are 8% - 2% and 2% correspondingly according to GAMMA-400 "Technical Project" stage results. Angular resolution is $\sim 5^o$ for low-energy gamma-quanta with energies 0.2 - 10 MeV in the lateral aperture obtained due individual detectors of CC2 count rate analysis only for non-stationary events (GRB, solar flares and so on). The applied method looks like BATSE (Burst And Transient Source Experiment) detector onboard Compton Gamma Rays Observatory algorithm for transient sources differ from occultation analysis technique - see [9] and references therein.

The telemetry downlink capability is 100 GByte/day while total onboard memory is 1 TByte. The GAMMA-400 launch date will be at the beginning of 2020s.

## 2. Triggers formation in the different apertures

The counting and triggers signals formation system starts the data acquisition and provides particle identification. It used 2 pulses types: fast (t≤10 ns) from plastic scintillation detectors and slow (t≤10 μs) from inorganic ones. Also fast pulses (t~10 ns) from amplitude discriminators of CsI(Tl)-based individual detectors of calorimeters CC1 and CC2 are included into this system information processing. These signals corresponded to various energy and amplitude thresholds allow onboard identification of several event types, for example gamma-quanta and charged particles (protons and electrons). The counting and triggers signals formation system generates 2 kinds of information: triggers itself with formation time ~50 ns that start detectors systems sampling and trigger markers – 32-bit codes characterised processed events using all detectors thresholds for both fast and slow signals. Trigger markers creates during ~20 μs using digital analysis of individual detectors amplitudes after analogue-to-digital conversions. The data acquisition system uses trigger markers to form event marker provided event recording into one of four data banks accordingly to corresponding event priority. The simplified scheme of GAMMA-400 telescope counting and triggers signals formation system operation is presented in the Fig. 2. Each presented at Fig. 2 table cell contains the special matrix for signal description mentioned detectors similar to one shown at Fig. 3. Only signals from each detectors system individual detecting units without any summation applied for particle identification. Counting and triggers signals used by GAMMA-400 detectors systems sampling and provide the registration of γ-quanta, high-energy electrons/positrons and nuclei.

Triggers in the main aperture will be formed using information about particle direction provided by TOF system (TOF signals matrix) and presence of charged particle or backsplash. The example of TOF and ACtop signals matrixes algorithm formation is presented at Fig. 3.

The backsplash existence flags formed due processing of BS1_ACtop and BS1_AClat signals obtained after analysis of energy deposition in combination of both layers individual detectors of TOF S1 section and anticoincidence systems ACtop and AClat ones correspondingly. Also the signal BS1t formed due to special algorithm of delayed on time Δt_BS backsplash presence recognition. The delay time Δt_BS depends of distance between ACtop and other elements in which backsplash produced (conversion foils, CsI(Tl) crystals and so on).

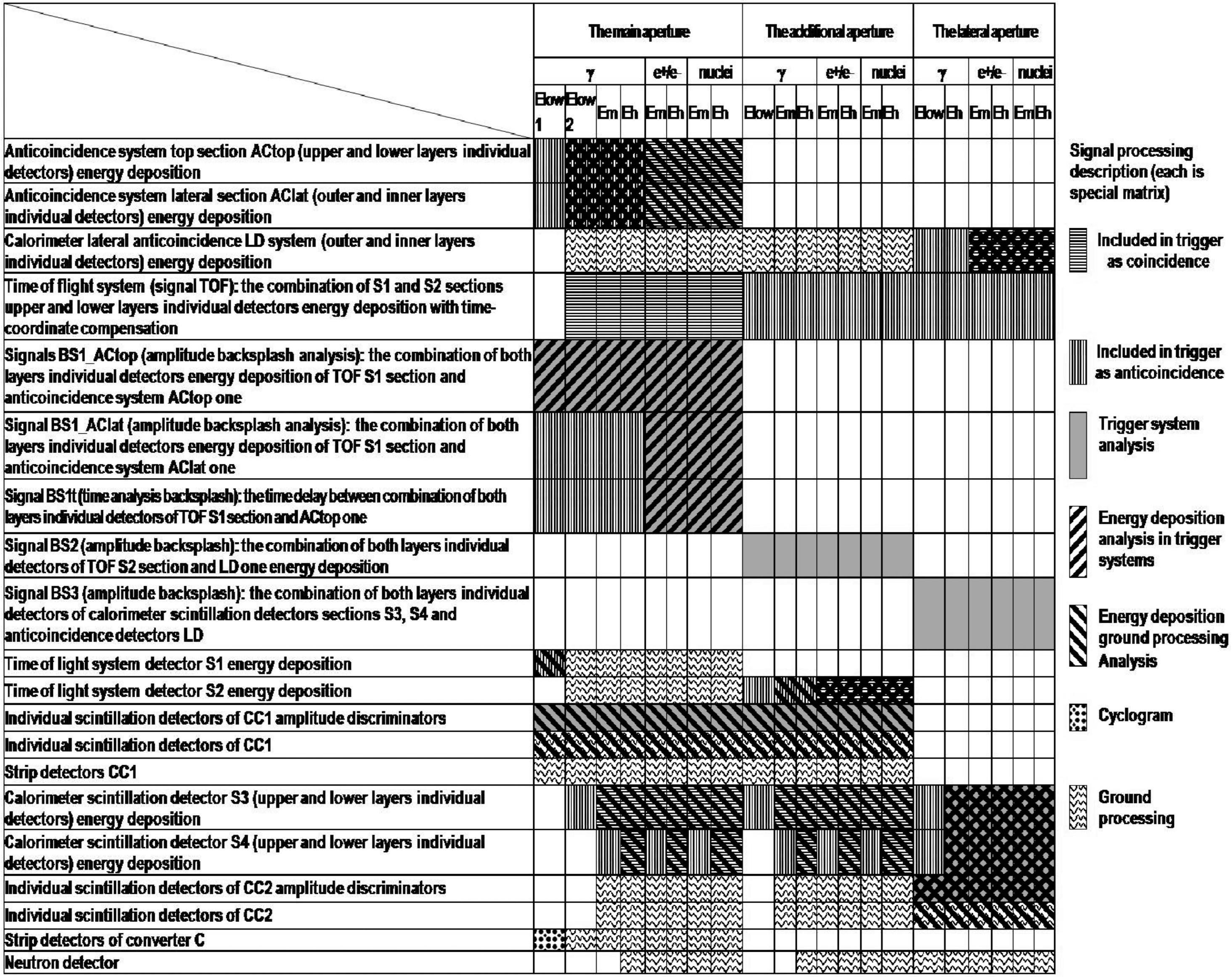


Fig. 2. The GAMMA-400 counting and triggers signals formation system simplified scheme.

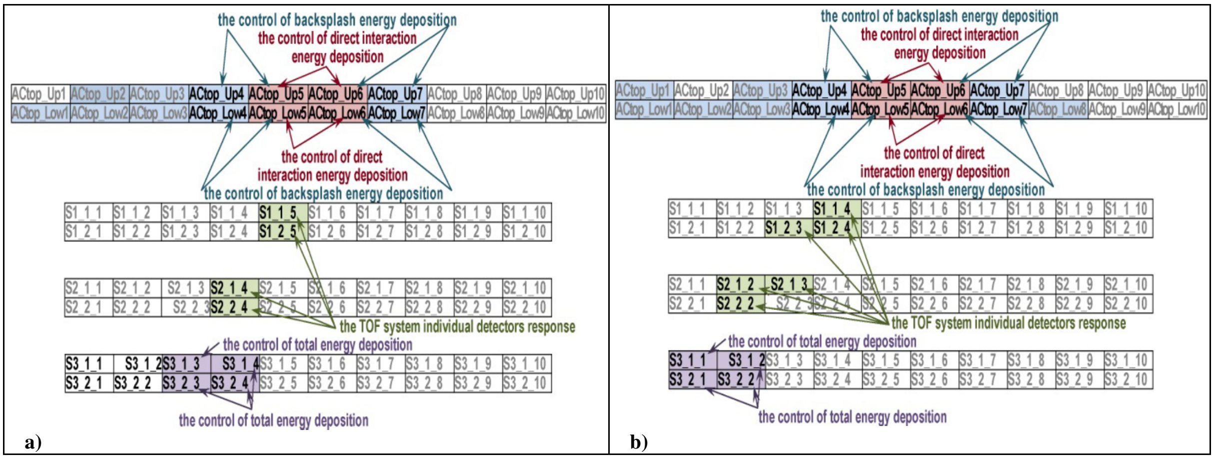


Fig. 3. Simplified schemes of special matrix for definition of whether particle is neutral or charged for events inside (a) and outside (b) of the main aperture. The detectors registered particle energy deposition marked by colors, the black letter marked devices sampled accordingly special matrix, the gray letter shown other detectors.

Backsplash mostly occurs in high-density media and probability of its production in supports based on polycarbonate honeycomb panels and plastic scintillators with average density of 0.004 g/cm$^3$ and 1.032 g/cm$^3$ correspondingly is less than 1%. The results of backsplash modeling are presented and discussed in the Section 3.

Gamma-quanta in the main aperture identified with absence of impinged particles corresponding signal in the AC taking into account methods of backsplash rejection specially designed for GAMMA-400, electrons (positrons) and nuclei recognizing by the signals corresponding to energy deposition in the individual detectors of AC, S1, S2, S3 and fast signals from CC1 individual detectors discriminators – the simplified algorithm illustration see at Fig. 2-3.

In the additional aperture the particles registration starts with signal of CC1 fast discriminators in anticoincidence with TOF pulse. Fast signals from detectors CC1 and S3 indicate up-down particle direction, anticoincidence in this aperture provides by S2, LD and S4. Particles identification is provided by analysis of signals corresponding to energy deposition in the individual detectors S2, S3 and fast signals from CC1 individual detectors discriminators – the simplified algorithm illustration see at Fig. 2.

Event detection in the lateral aperture begins with signal of CC2 individual detectors fast discriminators in anticoincidence with TOF pulse and CC1 individual detectors fast discriminators. Low energy (0.2 - 10 MeV) photons recognizing by using simple anticoincidence signals from the individual detectors of LD. Gamma-quanta of higher energies are identified using energy deposition in the individual detectors of LD, S3, S4 and fast signals from CC2 individual detectors discriminators – the simplified algorithm illustration see at Fig. 2.

## 3. Triggers and trigger markers thresholds modelling

The GAMMA-400 telescope consists of ~1500 detectors and ~10000 individual engineering elements (beams, fasteners, racks etc). Four position sensitive and two spectrometric detectors of the KONUS-FG gamma-ray burst monitor together with two star sensors and two magnetometers were included in the model too. The simulation software allows quickly and flexibly changes the detectors and structural elements of GAMMA-400 geometry in accordance to the newly developed drawings in CAD systems and import the 3D-model of geometry description (STL-files) into Geant4 environment by the pocket CADMesh [4]. This model permits obtaining physical data about particles interactions with all detectors and construction elements. Each part of detectors and construction elements can be declared as a sensitive volume and full set of particle tracking information stored for both primary and secondary particles. We have used this package for analyzing the influence of energy thresholds changes in counting and triggers signals formation system. 3D-model of gamma-telescope in the Geant4 environment is shown at Fig. 4.

The results of gamma-quanta energy deposition modeling in the ACtop layers for 7500 particles with energy 100 GeV are presented at Fig. 5. Most part of particles does not interact directly in ACtop. However ~ 3.9% of high energy photons produce pairs in ACtop upper layer at the same individual detector which it is impinged – see panel (a). Energy losses from pair components are registered in both this detector and one of ACtop lower layer located below. It gives non-zero energy deposition in ACtop upper layer and wide feature in the energy range 6 - 9 MeV in ACtop lower one. Pairs formed in the ACtop lower layer also produced non-zero energy deposition in this device. Panel (d) of Fig. 5 shows both non-interacted in the ACtop lower layer photons and the contributions of pair production in this layer with energy losses from formed in the ACtop upper one electrons and positrons. All these effects influenced to the total energy deposition in detectors are shown at panels (c) and (f) of this figure. The several cases of shower formations in both layers of AC individual detectors were obtained at modeled subset of $10^4$ gammas with E=100 GeV.

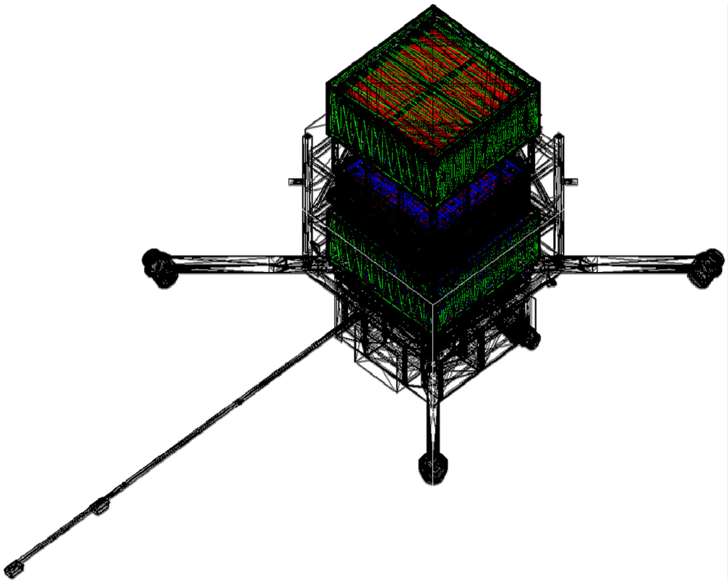

Fig. 4. Telescope GAMMA-400 mathematical model 3D-view in the Geant4 environment.

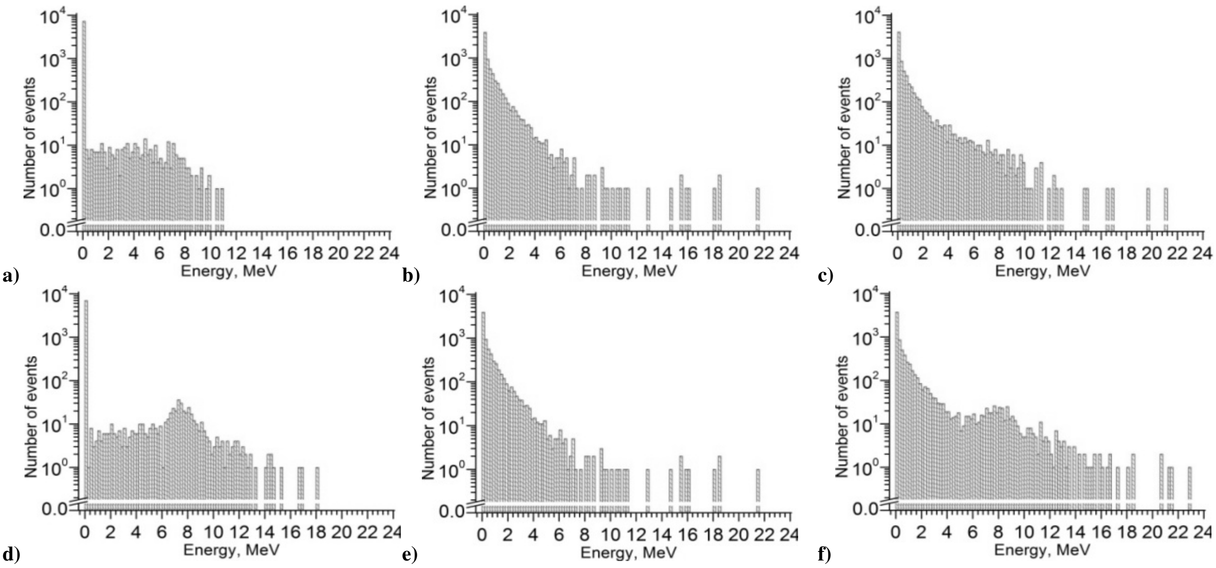


Fig. 5. Gamma-quanta energy deposition in ACtop for 7500 particles with energy 100 GeV. a) - c) upper layer, d) – f) lower layer. a) - for incident particles (the influence of pair production is well illustrated), b) - for backsplash from all detectors and construction elements, c) - total energy release, d) - for incident particles (the contributions of pair production in ACtop lower layer with energy losses from produced in ACtop upper layer electrons and positrons are seen more distinct ), e) - for backsplash from all detectors and construction elements, f )- total energy release.

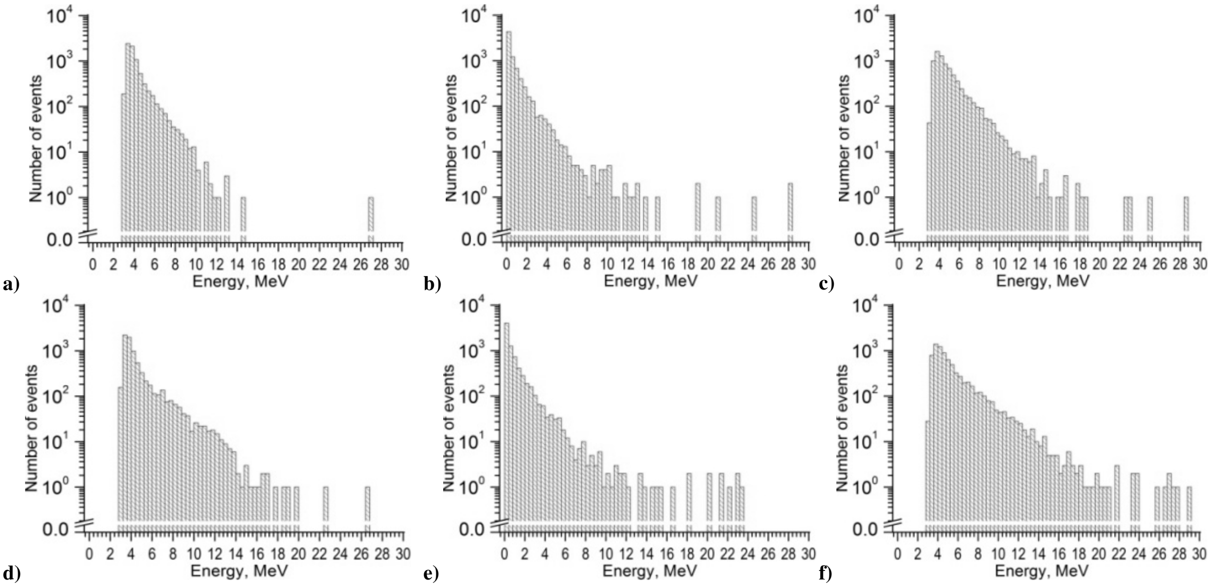


Fig. 6. Electrons energy deposition in the ACtop upper layer for 7500 particles with energy 100 GeV (a - for incident particles; b - for backsplash from all detectors and construction elements; c - total energy release) and lower one (d - for incident particles; e - for backsplash from all detectors and construction elements; f - total energy release).

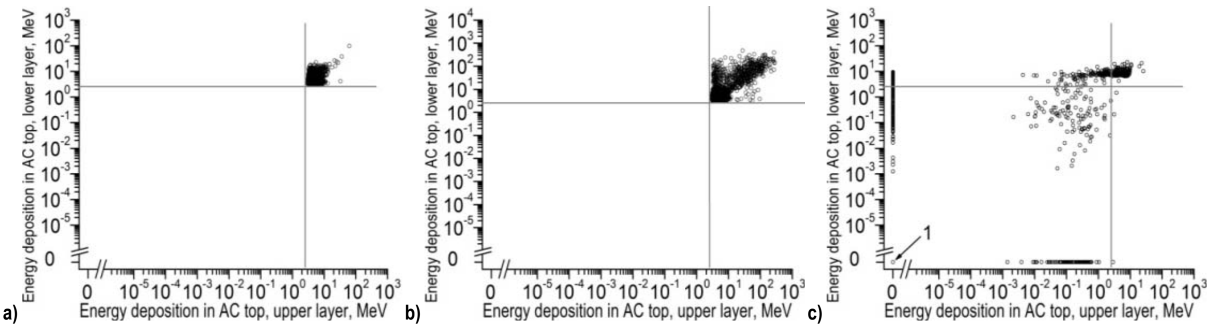


Fig. 7. Energy deposition in double layers ACtop for 100 GeV particles with backsplash subtraction using temporal analysis: a – protons, b – electrons, c – gamma-quanta (area marked (1) contain ~60% of events with energy deposition less than 1 keV in both ACtop layers).

Most part of backsplash produced in calorimeters (see panels (b) and (e) at Fig. 5 and Fig. 6.) and conversion foils is delayed at individual time $\Delta t\_BS$. Also at some situations backsplash formation region is located in ACtop lower layer just below of upper layer individual detector on which particle is impinged. It was found at modeling subsets of both gammas and electrons with $10^4$ simulated particles for E=100 GeV. The energy deposition in ACtop upper layer from such kind of events is less than 1 MeV. Mainly the backsplash particles tracks are outside ACtop detector system due to long distance between ACtop and calorimeters. Part of backsplash particles are absorbed in conversion foils, TOF detectors and all detectors' supports. Also the backsplash electrons could absorbed or produced photons in the first conversion foil and only sufficiently lower energy gamma component propagate through ACtop lower layer followed energy release in one less than 1 keV for 28% of gammas with E=100 GeV. However, in several of these cases, photons could interact in ACtop upper layer and total ACtop energy deposition is less than 1 keV only for 17% of photons. As well as in the first conversion foil the backsplash electrons could produced photons or absorbed in the ACtop lower layer. Therefore backsplash energy deposition in ACtop upper layer is less than 1 keV for 32% of gammas with E=100 GeV.

In GLAST Technical Handbook is written [10]: "Because GLAST's ACD is segmented, it can distinguish backsplash, because a backsplash-hit tile will generally not be in the area through which the gamma ray arrived ... the

ACD threshold can be operated at a higher level than EGRET's, also reducing backsplash vetoes." Nevertheless, pair production in the same detector particle's impinged and sufficient possibility of backsplash particle interaction in this detector caused several types of biases [11]. The most of such problems will not take place for instrument with double layer anticoincidence, sufficient long time-of-flight system distance between converter-tracker and calorimeter and triggers formation logic similar to algorithms used in the GAMMA-400 counting and triggers signals formation system.

Electrons energy deposition modeling results in the ACtop upper layer for 7500 particles with energy 100 GeV are shown at Fig. 6. The lower limit for the energy loss of electrons direct interaction is ~2.6 MeV. The same value for protons is ~2.9 MeV. These thresholds used only if TOF signals matrix analysis result corresponds to up-down high-energy particle moving inside the main aperture, i.e. particle's energy is enough for passing through all conversion foils in the converter-tracker and ~2$X_0$ of CsI(Tl) in CC1. Moreover, its track is necessarily passed both trough CC1 and CC2 as illustrated at Fig. 3a. Of course, other thresholds combinations can be used for lower energy particles. And for gamma-quanta with energy less than 200 MeV the trigger signal formation in the main aperture requires energy deposition in AC less than thresholds for low-energy electrons in both upper and lower layers.

The energy deposition distributions in ACtop upper layer and ACtop lower one are presented at Fig. 7 for electrons, protons and gammas taking into account backsplash rejection. Data analysis has shown for double-layer ACtop only 2.8 % photons will be wrongly recognized as electrons or protons taking into account both temporal and amplitude trigger marker examination methods during onboard analysis in the counting and triggers signals formation system. The part of charged particles mistakenly identified as gammas is ~$10^{-5}$ using described algorithms. It provides better signal to noise ratio than other instruments.

## 4. Conclusions

Gamma-telescope GAMMA-400 will be new generation satellite γ-telescope with better characteristics than existing instruments ones: angular resolution, data storage quota, energy resolution, detectors dead time. GAMMA-400 optimized for gamma-quanta, electrons and light nuclei with energy ~$1.0\times10^2$ GeV registration in the main aperture with the best parameters [4 - 6, 8]: the angular resolution ~0.01°, the energy resolution ~1%. The modelling results has shown for double-layer anticoincidence detectors that only 2.8% of photons can be wrongly recognized as electrons or protons taking into account both temporal and amplitude trigger marker examination methods during onboard analysis in the counting and triggers signals formation system. In combination of the proton rejection factor of ~$5\times10^5$ it provides better signal to noise ratio among other satellite experiments include Fermi/LAT. Taking into account weak background temporal variations due the high apogee orbit [4, 5] and new concept of counting triggers signals formation system, the gamma-telescope GAMMA-400 allows to provide detailed analysis of the sources luminosity variability (spectral, angular and temporal) and investigation of diffuse emission (angular and spectral inhomogeneity including ones caused by dark matter).

## References

[1]Ackermann M., Ajello M., Albert A. *et al.* The Fermi large area telescope on orbit: event classification, instrument response functions, and calibration. *ApJS*. 2012;203(1,ID.4):1-70.

[2]Nolan P.L., Abdo A.A., Ackermann M. *et al.* Fermi Large Area Telescope Second Source Catalog. *ApJS.* 2012;199(2,ID.31):1-46.

[3]Acero F., Ackermann M., Ajello M. *et al.* Fermi Large Area Telescope Third Source Catalog. *ApJS.* 2015;218(2,ID.23):1-41.

[4]Topchiev N.P., Galper A.M., Bonvicini V. *et al.* The GAMMA-400 experiment: Status and prospects. *Bull. Russ. Acad. Sci. Phys*. 2015;79(3):417–420.

[5]Topchiev N.P., Galper A.M., Bonvicini V. *et al.* GAMMA-400 gamma-ray observatory. arXiv:1507.06246.

[6]Galper A.M., Adriani O., Aptekar R.L. *et al.* Characteristics of the GAMMA400 Gamma-Ray Telescope for Searching for Dark Matter Signatures. *Bull. Russ. Acad. Sci. Phys*. 2013;77(11):1339–1342.

[7]Galper A.M., Adriani O., Arkhangelskaja I.V. *et al*. Status of the GAMMA-400. *Advances in Space Research.* 2013; 51:297-300.

[8]Leonov A.A., Galper A.M., Bonvicini V. *et al.* A separation of electrons and protons in the GAMMA-400 gamma-ray telescope. arXiv:1503.06657v1.

[9]Hakkila J. BATSE software for the analysis of the gamma ray burst spatial distribution. *Alabama Univ., Research Reports: 1990 NASA/ASEE Summer Faculty Fellowship Program 5 p.* 1990;SEE N91-18967 10-99.

[10]*The GLAST Technical Handbook.* Greenbelt: GLAST Science Support Center. 2007.

[11]*http://fermi.gsfc.nasa.gov/ssc/data/analysis/LAT_caveats_p7rep.html*.